18th International Conference
ENGINEERING MECHANICS 2012
Svratka, Czech Republic, May 14 – 17, 2012

pp. 1219–1228
Paper #63

USE OF ELECTRO-MAGNETIC DAMPING FOR VIBRATION CONTROL

G. J. Stein [*], R. Darula[**], S. Sorokin[**]

Abstract: *Vibration of machines is an unwanted phenomenon, and it is usually of interest to eliminate it. There are various means to be used in order to reach the goal, where the utilization of the electromagnet augmented by an external shunt circuit is analyzed in the paper. The magnetic force is used to introduce additional electromagnetic damping into vibrating mechanical system. The hysteretic losses and eddy currents are included in the model, to take into account more realistic dynamic behaviour of the system. The mathematical model of the controller is derived using lumped parameter approach. The parameters are assumed from an experimental set-up using and an industrial type of electromagnet. Considering the harmonic excitation of mechanical system, a steady-state response and performance of the controller is analyzed. Simulation results show the influence of introduced electromagnetic damping on the dynamical response of the system.*

Keywords: ***electromagnet, oscillatory system, damping, natural frequency detuning***

1. Introduction

In rotating machinery, the resonance phenomena can cause severe problems or even a failure of components. In order to avoid it, a vibration control need to be implemented, e.g.:

- Eliminating the coincidence of operation frequency with resonance;
- Introduction of mechanical damping.

Furthermore, active and semi-active methods of vibration control, i.e. capability to adjust the controller's properties, can be implemented in vibration reduction as well. Piezoelectric, electro-dynamic and electro-magnetic actuators are widely used for such a control strategy, as presented in (Bishop, 2002; Giurgiutiu & Lyshewski, 2009). Energy dissipation by a shunt circuit damper combined with piezoelectric elements is discussed in (Hagood & von Flotow, 1990; Giurgiutiu & Lyshewski, 2009; Preumont, 2011). In the vibration control of large machinery, utilization of piezoceramics is not an optimal choice, since the material is brittle and does not withstand large strains. Furthermore, the manufacturing costs and requirements on high voltage amplifiers are also drawbacks in large scale applications (Bishop, 2002; Giurgiutiu & Lyshewski, 2009).

On the other hand, electromagnetic and electrodynamic vibration controllers are capable to operate at larger amplitudes of vibration, too. Some applications of vibration control of cantilever beams using these elements are published by Gospodarič et al. (2007); Cheng & Oh (2009); Niu, Xie & Wang (2009); Brezina et al. (2011). The vibratory energy damping using an electromagnetic element connected to a shunt resistance is analyzed in Gospodarič et al. (2007), Niu et al. (2009), Brezina et al. (2011). Cheng & Oh (2009) use a set-up in which the current generated in a coil is dissipated by a shunt circuit, consisting of a battery of series RLC circuits. Utilization of the eddy currents damping in vibration control is explored in Sodano & Inman (2007).

This contribution, based on authors' previous work (Darula et al., 2011), analyses the electromagnetic actuation principle. It has been shown that the controller of interest is capable to

[*] Ing. George Juraj Stein, PhD.: Institute of Materials and Machine Mechancis, Slovak Academy of Sciences; Račianska 75; SK-83102 Bratislava 3; SR, e-mail: stein@savba.sk

[**] MSc. Radoslav Darula & Prof. Sergey Sorokin, DSc.: Department of Mechanical and Manufacturing Engineering, Aalborg University; Fibigerstraede 16; DK-9220 Aalborg East, DK, e-mail: dra@m-tech.aau.dk, svs@m-tech.aau.dk

introduce damping, as well as alter damped natural frequency of the oscillatory system. In order to model more realistic system, internal electrical losses are introduced, which were not considered in (Darula, *et al.*, 2011). It is shown that electrical losses significantly influence the system properties in respect to a loss-less system.

2. Concept of the vibration controller

The use of an industrial circular type electromagnet with a ferromagnetic yoke fixed by a spring-damper system, as shown in Fig. 1, is analyzed. A coil of N_W turns with a wire resistance R_W is energised by a direct current I_{DC} and it generates a static magnetic field. Exposing the yoke into vibration, described by a mechanical displacement $w(t)$, the air gap width $d(t)$ changes in time, which causes variation of an air gap reluctance.

According to Faraday's law (Fitzgerald et al., 2003), change in reluctance, i.e. a change of primary magnetic flux, is responsible for induction of alternating voltage $u_i(t)$ in the coil, where it forces a current $i_i(t)$ to flow in the electrical shunt circuit.

From the Lenz's law, the direction of $i_i(t)$ is opposite to I_{DC}, i.e. the magnetic field generated in the coil ($i_i(t)$ contribution) opposes the primary field generated by I_{DC}. Using the shunt resistance R_S, the current $i_i(t)$ is dissipated.

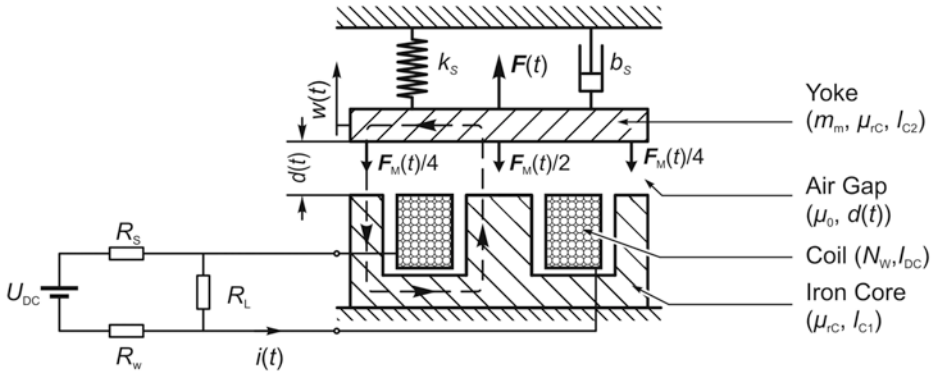

Fig. 1: Schematics of the analyzed electro-mechanical system (flux line is denoted dashed)

To extend the model derived in (Darula, et al., 2011), the material losses within the electrical circuit, which are supposed to influence the performance of the controller, are also taken into account:

1. *Hysteresis losses* in the core material,

2. *Eddy currents* in the core material.

As was shown in (Darula et al., 2012), the eddy current losses are frequency dependent.

The core loses can be modelled as a parallel loss resistance R_L to the electromagnet coil inductance (Fig. 1). Due to frequency dependence of losses, the resistance R_L is frequency dependent (Darula et al., 2012).

3. Simplified analysis of the electro-magnetic circuit

The magnetic system is modelled using a lamped parameter approach, where one can identify three elements (Fig. 2(a)):

- *Source of magnetic flux* – a coil of N_W turns energized with the current $i(t) = I_{DC} + i_i(t)$;

- *Air gap reluctance* ($\Re_{AG}$) – magnetic resistance caused by the air gap, where the width of air gap is $d(t)$ and the permeability of the free space μ_0;

- *Core reluctance* ($\Re_C$) – magnetic resistance of the iron core and armature with relative permeability μ_{rC}. From experimental results (Darula, 2008) a constant value of the permeability $\mu_{rC} \approx 500$ was estimated and used further. This is an acceptable simplification of the real situation.

From Ampere's law (e.g. in (Fitzgerald, et al, 2003)), assuming a constant core cross-section S_C, the magnetomotive force $F_\Phi(t)$:

$$F_\Phi(t) = \oint_C \vec{H} \cdot d\vec{l} = \left(\frac{l_C}{\mu_{rC}} + 2d(t) \right) \frac{B(t)}{\mu_0} = N_W \left[I_{DC} + i_i(t) \right] \tag{1}$$

where $\vec{H}$ is magnetic field intensity vector, $l = l_C + 2d(t)$ is total magnetic flux line path and $B(t)$ the magnetic field induction. Due to geometry of core and yoke of length l_C, the middle magnetic flux line is crossing twice the air gap of width $d(t)$, as seen from Fig. 1.

The source of DC voltage, U_{DC}, is assumed to be ideal, i.e. its internal resistance is neglected. The time variation of total magnetic flux $\Phi_T(w(t), i(t))$ in the coil is represented by the induced voltage $u_i(t)$. From Ohm's law we can write for the electric circuit (Fig. 2(b)):

$$U_{DC} + \frac{d\Phi_T(w(t),i(t))}{dt} = \left[\frac{(R_S + R_W)R_L}{R_S + R_W + R_L} \right] \left(I_{DC} + i_i(t) \right) \tag{2}$$

The total magnetic flux is in fact the induced voltage $u_i(t)$, as given by the Faraday's induction law (Bishop, 2002; Fitzgerald, et al, 2003; Giurgiutiu & Lyshewski, 2009):

$$u_i(t) = - \frac{d\Phi_T(w(t),i(t))}{dt} = - N_w S_w \frac{dB(t)}{dt} \tag{3}$$

where S_w is the coil winding cross-section and $B(t)$ is the time variable magnetic induction (magnetic field density) in the air gap.

From Eq. (2)-(3) can be concluded, that in the electric circuit of Fig. 2(b) two voltage sources are present acting in against each other. The circuit can be divided in respect to its behaviour into:

- the response to the DC voltage source: $U_{DC} = (R_s + R_w)I_{DC}$;
- the response to the induced AC voltage: $i_i(t) = u_i(t)/R_T(f)$, at given frequency f, where $R_T(f)$ is the bracketed term in Eq. (2), which is frequency dependent.

Since material losses are included in electrical circuit, the loss term in the magnetic model can be neglected, which simplifies derivations. Furthermore, neglecting also fringing effects (sufficiently small air gaps are assumed), the magnetic induction $B(t)$ can be derived from Eq. (1):

$$B(t) = \frac{\mu_0}{2d_0} \frac{N_w \left[I_{DC} + i_i(t) \right]}{\left[(1 + \delta) + \varepsilon(t) \right]} \tag{4}$$

using scaling coefficients $d_C = l_C/(2\mu_{rC})$, $\varepsilon = [d(t) - d_0]/d_0$, $\delta = d_C/d_0$. The parameter d_0 represents the static air gap width for a defined I_{DC}. To make the problem tractable, let us assume further $|w(t)| << d_0$, i.e. $|\varepsilon(t)| << 1$.

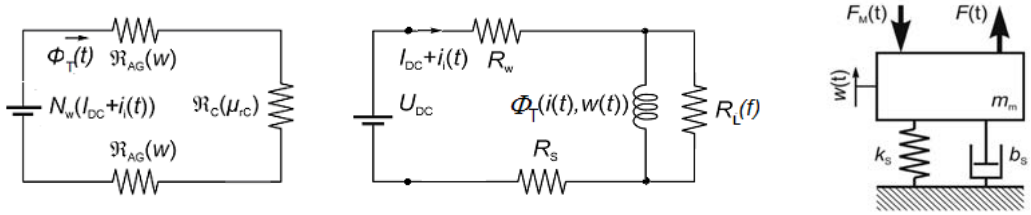

(a) *(b)* *(c)*

Fig. 2:(a) magnetic loop, (b) equivalent electric circuit, (c) mechanical system

In the static case, i.e. $i_i(t) = 0$ and $\varepsilon(t) = 0$, the static magnetic field in the air gap becomes:

$$B_0(I_{DC}, d_0) = \frac{\mu_0}{2d_0} \frac{N_w I_{DC}}{(1 + \delta)} \tag{5}$$

which is function of both the air gap width d_0, as well as the magnetising DC current I_{DC}.

Assuming a harmonic excitation of mechanical system, a steady state response of the system is of interest. The analysis of a transition phase is beyond the scope of this article. The steady-state is governed by two time variables:

- the air gap width $\varepsilon(t)$, which influences reluctance in the magnetic circuit;

- induced current $i_i(t)$, due to magnetic field variation.

As was derived for a similar electromagnetic system in (Darula et al., 2011), assuming $|i_i(t)| << I_{DC}$ and $|\varepsilon(t)| << 1$, the dynamical response of the electro-magnetic system can be expressed combining Eqs. (2) to (4) as:

$$\frac{d^2B(t)}{dt^2}\left[\frac{\mu_0 N_w^2 S_w}{2d_0(1+\delta)}\right]\frac{1}{R_T}+\frac{dB(t)}{dt}=-\frac{B_0}{(1+\delta)}\dot{\varepsilon} \tag{6}$$

where the term in the square bracket is inductance L_0 of the electromagnet coil with the ferromagnetic core at air gap of width d_0.

4. Calculation of the acting magnetic force

The electromagnetic force, called the Maxwell's pulling force, is given (Bishop, 2002; Fitzgerald, et. al., 2003; Giurgiutiu & Lyshewski, 2009; Meyer & Ulrych, 2009):

$$F_M(t)=2\cdot\frac{1}{\mu_0}B^2(t)S_C \tag{7}$$

The magnetic pulling force is acting through the central part of the core of cross-section S_C, as well as through the torus of the pot-type core, assumed to have the same cross-section. Substituting the expression for $B(t)$ from Eq. (4) and introducing the inductance L_0 from Eq. (6), following holds:

$$F_M(d(t),I_{DC},i_i(t)) = \frac{(1+\delta)L_0}{N_w^2 d_0}\frac{F_\Phi(t)^2}{\left[(1+\delta)+\varepsilon(t)\right]^2} \tag{8}$$

From Eq. (8), the quadratic dependence of the electromagnetic force on the magnetomotive force $F_\Phi(t)$ (Eq. (1)), i.e. on the total current flowing in the electrical circuit, $i_T(t) = I_{DC} + i_i(t)$, can be noticed. It is also inversely proportional to the square of the dynamic relative air gap $\varepsilon(t)$. As pointed out in Stein, et al (2011), there is a limit in the magnetic pulling force extent. If the total current $i_T(t)$ exceeds a critical value I_C, dependent on mechanical configuration, the magnetic pulling force would dominate over the elastic force. This would result in full attraction of the yoke to the electromagnet and the oscillatory motion would hence cease. Further, despite the difference in the areas S_w (cross-section of coil) and S_c (cross-section of core), it can be stated that the most of the magnetic flux is flowing through the ferromagnetic core because the magnetic resistance of the air, $2\times\Re_{AG}$ is μ_{rC}, i.e. 500–times larger than that one of the core, $\Re_C$. Hence, the ratio $\sigma = S_C/S_w \approx 1$.

In order to solve Eq. (8) analytically, it is advantageous to apply linearization in the vicinity of the operation point using first two terms of a power series. Hence:

$$F_M(\varepsilon(t),I_{DC},i_i(t))\approx\frac{L_0}{N_w^2 d_0(1+\delta)}F_\Phi(t)^2-\frac{2L_0}{N_w^2 d_0(1+\delta)^2}F_\Phi(t)^2\varepsilon(t) \tag{9}$$

The magnetomotive force is given by applying fundamental electromagnetic laws of Eqs. (1) and (3):

$$F_\Phi(t)=N_W\left[I_{DC}+i_i(t)\right]=N_W\left[I_{DC}-\frac{N_w S_w}{R_T}\frac{dB(t)}{dt}\right] \tag{10}$$

where for the magnetic induction, a total time derivative of Eq. (6) has to be substituted.

In further analysis, let us focus to the frequency domain, which can provide more information about dynamic response then time domain can. Therefore, let us introduce the respective phasor representation in respect to a supposed harmonic excitation force $\widetilde{F}=F_0e^{j\omega_a t}$, where ω_a represents angular frequency. Then:

$$\widetilde{F}_{\Phi} = N_{\mathrm{W}}\left[I_{\mathrm{DC}} - \frac{\mathrm{j}\omega N_{\mathrm{w}} S_{\mathrm{w}}}{R_{\mathrm{T}}(\omega)}\widetilde{B}\right] \tag{11}$$

Substituting the dynamic magnetic induction phasor $\widetilde{B} = B_D e^{j\varphi_{\mathrm{B}}}$ and the relative air gap width phasor $\widetilde{E}e^{\mathrm{j}\omega t} = \varepsilon_0 e^{\mathrm{j}\varphi_{\varepsilon}} e^{\mathrm{j}\omega t}$ into Eq. (6) and some re-arrangement following is valid:

$$\widetilde{B} = -\frac{B_0}{(1+\delta)\left[R_{\mathrm{T}}(\omega) + \mathrm{j}\omega L_0\right]}\widetilde{E} \tag{12}$$

which is the relationship between $\varepsilon(t)$ (the relative air gap) and the $B(t)$ (the induced magnetic field in the air gap due to yoke vibrations), expressed in the complex (phasor) form.

Substituting Eq. (12) into Eq. (11) the magnetomotive force becomes:

$$\widetilde{F}_{\Phi} = N_{\mathrm{W}} I_{\mathrm{DC}}\left[1 + \frac{\mathrm{j}\omega L_0}{(1+\delta)\left(R_{\mathrm{T}}(\omega) + \mathrm{j}\omega L_0\right)}\widetilde{E}\right] \tag{13}$$

Having expressed the magnetomotive force in the complex form, Eq. (13) can be inserted into Eq. (9) transformed into the complex plane. This allows to introduce a complex magnetic force phasor $\widetilde{F}_{\mathrm{MT}}$. According to Eqs. (8) and (9), the magnetic force is proportional to square of the magnetomotive force F_{Φ}. Therefore, the magnetic force phasor will contain also higher harmonics of ω_{a}. This is a well known phenomenon in electrical engineering (Bishop, 2002; Fitzgerald, et al., 2003; Giurgiutiu & Lyshewski, 2009; Mayer & Ulrych, 2009). Hence:

$$\widetilde{F}_{\mathrm{MT}} = \sum_{n=0}^{\infty}\widetilde{F}_{\mathrm{M}n}e^{\mathrm{j}n\omega_{\mathrm{a}}t} = \frac{L_0}{N_{\mathrm{w}}^2 d_0(1+\delta)}\widetilde{F}_{\Phi}^{\,2} - \frac{2L_0}{N_{\mathrm{w}}^2 d_0(1+\delta)^2}\widetilde{F}_{\Phi}^{2}\cdot\widetilde{E}e^{\mathrm{j}\omega_{\mathrm{a}}t} \tag{14}$$

with:

$$\left(\widetilde{F}_{\Phi}\right)^2 = \left(N_{\mathrm{w}}^2 I_{\mathrm{DC}}^2\right)\cdot\left[1 + \frac{2\mathrm{j}\omega_{\mathrm{a}}L_0}{R_{\mathrm{T}}(\omega) + \mathrm{j}\omega_{\mathrm{a}}L_0}\widetilde{E}e^{\mathrm{j}\omega_s t} - \frac{\omega_{\mathrm{a}}^2 L_0^2}{\left(R_{\mathrm{T}}(\omega) + \mathrm{j}\omega_{\mathrm{a}}L_0\right)^2}\left(\widetilde{E}\right)^2 e^{2\mathrm{j}\omega_s t}\right] \tag{15}$$

The components of the total magnetic force under harmonic excitation emerge by explicitly expressing the particular low order components:

- *A static component* for $n = 0$:

$$F_{\mathrm{M0}} = \frac{L_0}{d_0(1+\delta)}I_{\mathrm{DC}}^2 \tag{16}$$

- *A component at the angular frequency* ω_{a} ($n = 1$):

$$\widetilde{F}_{\mathrm{M1}} = -\frac{2L_0 I_{\mathrm{DC}}^2}{d_0(1+\delta)^2}\left[1 - \frac{\mathrm{j}\omega_{\mathrm{a}}L_0}{R_{\mathrm{T}}(\omega) + \mathrm{j}\omega_{\mathrm{a}}L_0}\right]\cdot\widetilde{E} \tag{17}$$

- *A second harmonic component* at the angular frequency $2\times\omega_{\mathrm{a}}$ ($n = 2$):

$$\widetilde{F}_{\mathrm{M2}} = -\frac{L_0 I_{\mathrm{DC}}^2}{(1+\delta)^3}\left\{\frac{5\omega_{\mathrm{a}}^2 L_0^2 R_{\mathrm{T}}^2 + 3\omega_{\mathrm{a}}^4 L_0^4}{\left(R_{\mathrm{T}}^2(\omega_{\mathrm{a}}) + \omega_{\mathrm{a}}^2 L_0^2\right)^2} - 2\mathrm{j}\frac{R_{\mathrm{T}}(\omega_{\mathrm{a}})\omega_{\mathrm{a}}L_0}{\left(R_{\mathrm{T}}^2(\omega_{\mathrm{a}}) + \omega_{\mathrm{a}}^2 L_0^2\right)}\right\}\cdot\left|\widetilde{E}\right|^2 \tag{18}$$

which is coupled to mechanical motion by excitation amplitude ε_0^2.

- *Higher order harmonic components* being of the order of $|\varepsilon|^{\mathrm{n}}$, where $n \geq 3$. Because of $|\varepsilon| < 1$, these can be neglected.

5. Simplified analysis of the coupled system in the complex plane

Let us analyse the static deflection of the analysed SDOF oscillatory system loaded by the mass of the yoke of mass m_m (Fig. 1). The yoke is at a distance d_0* from the upper plane of the de-energised electromagnet core. Energizing the electromagnet by the DC current I_{DC}, the exerted static magnetic force F_{M0} elongates the spring further and a static equilibrium position in the distance d_0 is attained. Equilibrium is described as (Bishop, 2002; Rao, 2004):

$$(d_0^* - d_0)k_s = F_{M0}(I_{DC}, d_0) = \frac{L_0}{d_0(1+\delta)} I_{DC}^2 \tag{19}$$

If an external excitation force $F_E(t)$ of harmonic course, described as $F_E(t) = F_{E0}\sin(\omega_a t)$, is acting onto the mass m_m additional dynamic components of the Maxwell's pulling force F_{Mi} come into action. Then the equation of motion of the SDOF oscillatory system (Fig. 2(c)) is (Darula, et al., 2011):

$$m_m \frac{d^2 w(t)}{dt^2} + b_S \frac{dw(t)}{dt} + k_S w(t) = F_E(t) - F_{Mi}(t) \tag{20}$$

Lets turn into the complex domain, i.e. let us describe the external harmonic excitation $F_E(t)$ by the complex force phasor $\widetilde{F} = F_0 e^{j\omega_a t}$. The steady state response is of interest, i.e. all transient phenomena (electric and mechanic) are extinct. The response is assumed to be harmonic with the same angular frequency ω_a, i.e. the complex relative air gap width in the form $\widetilde{E}e^{j\omega_a t} = \varepsilon_0 e^{j\varphi_\varepsilon} e^{j\omega_a t}$. Then, Eq. (20) in non-dimensional form becomes:

$$\left[1 - \Omega^2 + 2j\xi_S\Omega\right]\widetilde{E}e^{j\omega_a t} = \frac{\widetilde{F}e^{j\omega_a t}}{k_s d_0} - \sum_{i=1}^{2} \frac{\widetilde{F}_{Mi} e^{j\omega_a i t}}{k_s d_0} \tag{21}$$

where:

- $\Omega = \omega_a/\omega_0$ is the non-dimensional frequency scaled with respect to natural frequency of the mechanical system;
- $\omega_0^2 = k_S/m$ is the square of the natural frequency of the SDOF mechanical system;
- $\xi_S = b_S/b_C$ is the damping ratio, where $b_C = 2\sqrt{k_s m}$ is the critical damping coefficient,
- $\widetilde{F}_{M1}$ and $\widetilde{F}_{M2}$ are the above derived first and second harmonics of the magnetic force.

The left hand side of Eq. (21) represents the oscillation of a general SDOF system, i.e. without action of any external forces. The external forces (excitation and magnetic force components) are on the right hand side of the equation.

Let analyze just the influence of the first harmonics of magnetic force (Eq. (17)) on the dynamics of the coupled system. The influence of the first harmonics is by far the largest and the most important. The influence of the higher harmonics is acknowledged; however will not be analysed. By introducing the formula into Eq. (21) and re-arranging, following is obtained:

$$\left[1 - \Omega^2 + 2j\xi_S\Omega\right]\widetilde{E}e^{j\omega_a t} = \frac{\widetilde{F}e^{j\omega_a t}}{k_s d_0} + \frac{1}{k_s}\left(\frac{2L_0 I_{DC}^2}{d_0^2(1+\delta)^2}\right)\left[1 - \frac{j\omega_a L_0}{R_T(\omega_a) + j\omega_a L_0}\right]\cdot \widetilde{E}e^{j\omega_a t} \tag{22}$$

The term in round parenthesis on the right-hand-side has a physical dimension of N/m, i.e. from mechanical point of view it represents a 'stiffness' associated with the static magnetic field, k_M:

$$k_M = \frac{2L_0}{d_0^2(1+\delta)^2} I_{DC}^2 = \frac{\mu_0 S_c N_w^2 I_{DC}^2}{d_0^3(1+\delta)^3} = \frac{F_{M0}(I_{DC}, d_0)}{d_0(1+\delta)} \tag{23}$$

Taking a dimension-less ratio of the magnetic field stiffness k_M to the mechanical stiffness k_s, $\kappa = k_M/k_s$, Eq. (22) is modified to become:

$$\left[1-\Omega^2+2\mathrm{j}\Omega\xi_\mathrm{S}-\kappa\frac{R_\mathrm{T}(\omega_\mathrm{a})}{R_\mathrm{T}(\omega_\mathrm{a})+\mathrm{j}\omega_\mathrm{a}L_0}\right]\widetilde{E}=\frac{\widetilde{F}}{k_\mathrm{s}d_0} \tag{24}$$

The left hand-side of Eq. (24) resembles the linear second order operator of Eq. (21), albeit with the addition of the last term, containing all the electrical parameters. After further re-formulation:

$$\left[\left(1-\kappa\frac{R_\mathrm{T}^2(\omega_\mathrm{a})}{R_\mathrm{T}^2(\omega_\mathrm{a})+\omega_\mathrm{a}^2L_0^2}\right)-\Omega^2+2\mathrm{j}\Omega\left(\xi_\mathrm{S}+\frac{\kappa}{2}\frac{R_\mathrm{T}(\omega_\mathrm{a})\cdot\omega_0L_0}{R_\mathrm{T}^2(\omega_\mathrm{a})+\omega_\mathrm{a}^2L_0^2}\right)\right]\widetilde{E}=\frac{\widetilde{F}}{k_\mathrm{s}d_0} \tag{25}$$

with:

$$\kappa=\frac{k_\mathrm{M}}{k_\mathrm{s}}=\frac{1}{k_\mathrm{s}}\cdot\frac{F_{M0}(I_\mathrm{DC},d_0)}{d_0(1+\delta)}=\frac{1}{k_\mathrm{s}}\cdot\frac{2L_0}{d_0^2(1+\delta)^2}I_\mathrm{DC}^2 \tag{26}$$

The derived equations are valid for any excitation angular frequency ω_a in the working range of the vibration controller. Further the coil reactance at angular frequency ω_0, $X_0=\omega_0\cdot L_0$ can be introduced and related to the total circuit ohmic resistance R_T in the following way:

$$\left\{\left[1-\kappa\cdot\frac{1}{1+\Omega^2\left(\frac{X_0}{R_\mathrm{T}}\right)^2}\right]-\Omega^2+2\mathrm{j}\Omega\left[\xi_\mathrm{S}+\frac{\kappa}{2}\cdot\frac{\left(\frac{X_0}{R_\mathrm{T}}\right)}{1+\Omega^2\left(\frac{X_0}{R_\mathrm{T}}\right)^2}\right]\right\}\widetilde{E}=\frac{\widetilde{F}}{k_\mathrm{s}d_0} \tag{27}$$

The complicated formula on the left hand side of Eq. (27) is the complex displacement transmissibility of the coupled system, $\widetilde{G}(\Omega)$, which has to be compared with the displacement transmissibility of the original, purely mechanical system, which is described by the left hand side of Eq. (21).

Comparing Eq. (27) with the left hand side of Eq. (21) we may conclude:

- The natural frequency of the modified oscillatory system (first left-hand-term term of Eq. (27)) is influenced by the electrical parameters of the electric circuit – total circuit resistance R_T and coil reactance X_0; by the static air gap width d_0 and by the magnetising DC current I_DC. The equivalent natural angular frequency of the coupled system is lower than the natural angular frequency ω_0 of the original (purely mechanical) one system. Hence de-tuning occurs, whose extent is controlled by the I_DC magnitude, entering the dimension-less variable κ, and by shunt resistance R_S, embedded in the total circuit resistance R_T;
- Additional damping is introduced to the mechanical system damping ξ_s, described by the last term in the left-hand-side of Eq. (27), which is controlled by the I_DC, R_S and X_0, too. The last term consists of the original system damping ratio ξ_s and an additional damping ratio, which can be termed additional 'electro-magnetic damping ratio' ξ_EM:

It is seen that the properties of the electrical components of the system markedly influence its vibration control performance. The total circuit resistance $R_\mathrm{T}(f)$ has already been introduced in Eq. (2), after Fig. 2(c):

$$R_\mathrm{T}(f)=\frac{(R_\mathrm{S}+R_\mathrm{W})R_\mathrm{L}(f)}{R_\mathrm{S}+R_\mathrm{W}+R_\mathrm{L}(f)}, \tag{28}$$

where the coil losses resistance R_L is assumed, following the results presented in Darula et al. (2012):

$$\frac{1}{R_\mathrm{L}(I_\mathrm{DC},d_0,f)}=\frac{1}{R_\mathrm{E}}+\frac{1}{R_\mathrm{H}(f)}, \tag{29}$$

where parameters R_E, representing the eddy current loses and R_H the hysteretic losses, which are linearly frequency dependent ($R_\mathrm{H}(f)=\gamma f$). The parameters were estimated from experiments (Darula, 2008). Estimation of numerical values of the parameters is presented in Darula et al. (2012). Then:

$$\frac{1}{R_{\mathrm{T}}(R_{\mathrm{S}},f)}=\frac{1}{R_{\mathrm{w}}+R_{\mathrm{S}}}+\frac{1}{R_{\mathrm{E}}}+\frac{1}{R_{\mathrm{H}}(f)} \tag{30}$$

In formula (30) just the shunt resistance R_S is available for control.

After substitution of expression (30) into Eq. (27), the extent of de-tuning and additional electro-magnetic damping can be quantified. The above obtained formulas can be illustrated in graphical form using the Matlab® simulation environment. The simulation is done for a particular case, addressed in Darula (2008): inductance $L_0 = 4.95$ H for air gap width $d_0 = 0.75$ mm. The loss properties of the electromagnet coil were identified in Darula et al. (2012). Following values were used: DC winding resistance $R_w = 34.9$ Ω; eddy current losses $R_{eE} = 1000$ Ω; hysteresis losses constant $\gamma = 90$ Ω/Hz. The equivalent mechanical system properties were assessed as $m_m = 51.7$ kg (load + joke mass); $k_s = 3.25\times10^6$ N/m and damping ratio $\xi = 0.025$. This leads to the natural frequency $f_0 = 39.9$ Hz ($\omega_0 = 250.7$ rad/s, $\Omega = 1.00$). The excitation force amplitude is set at 20 N and the excitation frequency is varied by ± 20 % from the mechanical system natural frequency to visualise the variation in the resonance peak position on the frequency axis due to the electro-magnetic influence. The shunt resistance R_S was varied from the value $R_S = 0$ Ω (short circuited coil), up to $R_S = 1\times10^6$ Ω (1 MΩ). A three-dimensional map of the FRF modulus dependence $\left|\widetilde{G}(\Omega)\right|$ on the R_S value is depicted in Fig. 3.

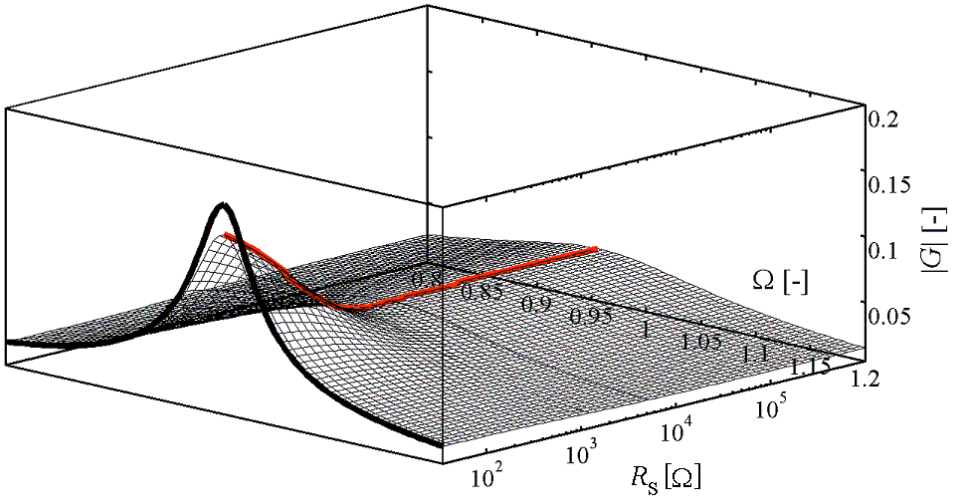

Fig. 3: Three-dimensional surface map of the FRF displacement modulus in respect to Ω and R. In bold the FRF of the sole mechanical part; in red the course of the FRF maximum, corresponding to the de-tuned natural frequency of the coupled system as a function of R_s

The bold black curve is the displacement FRF of the oscillatory system without the electromagnet, while the red curve indicates the variation of the FRF peak maximum, corresponding to the de-tuned frequency ratio Ω in respect to changing R_S in the range (0 Ω, 1 MΩ) (on a logarithmic scale).

It is interesting to assess the extent of de-tuning and displacement FRF attenuation in respect to the variation of the shunt resistance R_S. In Fig. 4(a) the dependence of the frequency ratio Ω is depicted; while in Fig. 4(b) the modulus of the coupled system $\left|\widetilde{G}\right|$ is presented. From both figures it is seen, that the extent of de-tuning is not large, attaining at most $\Omega = 0.955$ ($f_{D0} = 38.1$ Hz) for $R = 1$ MΩ ~ infinity, while for a more realistic value of $R_S = 5$ kΩ the de-tuning is to $\Omega = 0.965$ ($f_{D0} = 38.5$ Hz). The attenuation of displacement transmissibility for this particular case is from $G_0 = 0.1641$ (for the solely mechanical system) to $G_{inf} = 0.0447$ for $R = 1$ MΩ, or $G_R = 0.0470$ for the shunt resistance $R_S = 5$ kΩ. This is a 3.49–fold attenuation at the damped natural frequency of the original system, or by some 10.9 dB. The utmost attenuation for $R = 1$ MΩ would be 3.67–times, i.e. by 11.3 dB. From Fig. 4 it is seen, that the influence of the shunt resistance above some value to the vibration attenuation, as well as to the extent of the de-tuning is limited. This is due to the fact, that the resistance R_S is connected in parallel to the coil internal loss resistance R_e (see Eq. (30)) and so cannot

influence much the total resistance R_T by increasing the value of R_S to infinity. The obtained results are quite different from those for a system with neglected electromagnet losses, as presented, e.g. by Darula et al. (2011).

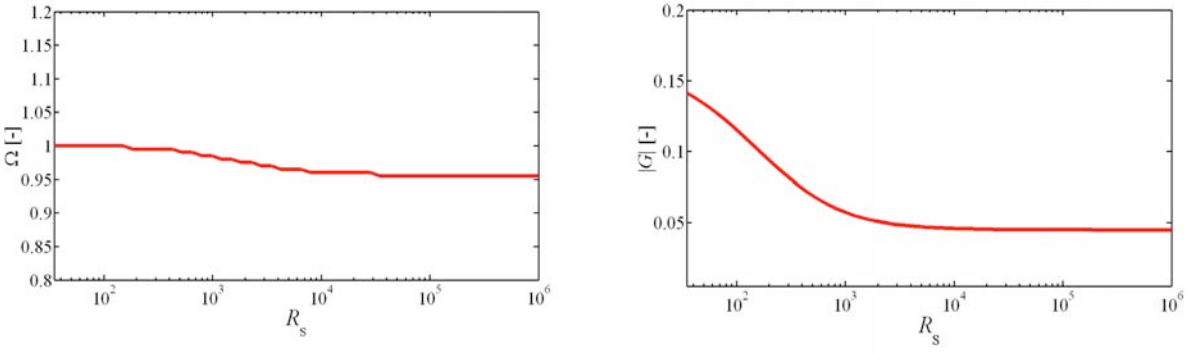

(a) (b)

Fig. 4: Dependence of: (a) detuned frequency ratio Ω and (b) FRF displacement modulus $|G|$ on R_S

6. Conclusion

An electro-magneto-mechanical system for vibration control of an SDOF oscillatory system, subject to external harmonic excitation, was analysed in a simplified, linearised form. The fundamental equation of motion (Eq. (25)) was derived, which includes the non-linear magnetic force (Maxwell's pulling force), described by Eqs. (9) and (10). The extra magnetic force causes:

- Generation of higher harmonics,
- Change (decrease) in oscillatory system natural frequency, i.e. de-tuning of the system,
- Inclusion of additional electro-magnetic damping, so decreasing the vibration transmissibility. The attainable extent of the de-tuning and of the additional electro-magnetic damping was illustrated for a particular case using parameters determined experimentally for an industrial electromagnet. It is markedly limited by the electrical parameters (coil inductance, and equivalent loss resistance) of the electromagnet.

Acknowledgement

This contribution is a result of the project No. 2/0075/10 of the Slovak VEGA Grant Agency for Science and InterReg IV A – 'Silent Spaces' Project, whose one Partner is Aalborg University.

References

Bishop, R.H., ed. (2002) *The Mechatronics Handbook*. CRC Press, Boca Raton.

Brezina, T., Vetiska, J., Hadas, Z. & Brezina, L. (2011) Simulation Modelling and Control of Mechatronic Systems with Flexible Parts, in: *Proc. 9th Int.Conf. Mechatronics 2011* (R. Jablonski & T.Brezina eds), Springer Verlag, Berlin, pp. 569-578.

Darula, R. (2008). *Multidisciplinary Analysis and Experimental Verification of Electromagnetic SAVC*. Masters Thesis. IME, Aalborg University, Aalborg.

Darula, R., Stein, G.J., Kallesøe, C.S. & Sorokin, S. (2012) Identification and Mathematical Modelling of the Electromechanical Vibration Controller, in: *Proc. 11th Int.Conf. ESDA 2012*, submitted.

Darula, R., Stein, G.J. & Sorokin, S. (2011) An Application of Electromagnetic Induction in Vibration Control, in: *Proc.10th Int.Conf. ICoVP 2011* (J. Naprstek, et al. eds), TU Liberec, Liberec, pp. 447-453.

Fitzgerald, A.E., Kingsley. Ch. & Umans, S.D. (2003) *Electric Machinery*, 6th ed. McGraw-Hill, Boston.

Giurgiutiu, V. & Lyshewski, S.E. (2009) *Micromechatronics: Modeling, Analysis and Design*, 2nd ed. CRC Press, Boca Raton.

Gospodarič, B., Vončina, D. & Bučar, B. (2007) Active electromagnetic damping of laterally vibrating ferromagnetic cantilever beam. *Mechatronics* 17, 6, pp. 291-298.

Hagood, N. & von Flotow, A. (1991) Damping of structural vibration with piezoelectric materials and passive electrical networks. *Journal of Sound and Vibration*, 146, 2, pp. 243-268.

Cheng, T.-H. & Oh, I.-K. (2009) A current-flowing electromagnetic shunt damper for multi-mode vibration control of cantilever beams. *Smart Materials and Structures*, 18, 9, art.no. 095036 (10pp).

Mayer, D. & Ulrych, B. (2009) *Elektromagneticke aktuatory (Electromagnetic actuators - in Czech)*. BEN, Prague.

Niu, H. X., Xie, S. & Wang, P. (2009) A new electromagnetic shunt damping treatment and vibration control of beam structures. *Smart Materials and Structures*, 18, 4, art.no. 045009 (15pp).

Preumont, A. (2011) *Vibration Control of Active Structures,* 3rd ed. Springer, Berlin.

Rao, S.S. (2004) *Mechanical Vibrations*, 4th ed. Pearson, Upper Saddle River.

Sodano, H.A. & Inman, D.J. (2007) Non-contact vibration control system employing an active eddy current damper. *Journal of Sound and Vibration*, 305, 4-5, pp.596-613.

Stein, G.J., Darula, R. & Chmúrny, R. (2011) A clamped-clamped beam static sag limits under perpendicular magnetic force, in: *Proc.17th Int.Conf. Engineering Mechanics 2011*, (V. Fuis ed), IT ASCR, pp.567-571.